IGARSS 2020 - 2020 IEEE International Geoscience and Remote Sensing Symposium | 978-1-7281-6374-1/20/$31.00 ©2020 IEEE | DOI: 10.1109/IGARSS39084.2020.9323175

ANALYSIS OF GNSS-R COVERAGE BY A REGIONAL AIRCRAFT FLEET

Ryan Linnabary[1], Andrew O'Brien[1], Chris Ruf[2], Stephen Musko[2], Delwyn Moller[3]

[1]The Ohio State University, Columbus, OH, USA
[2]University of Michigan, Ann Arbor, MI, USA
[3]University of Auckland, Auckland, New Zealand

ABSTRACT

Airborne GNSS-R instrument systems are typically only utilized for a limited number of aircraft flights to perform experiments, to test new instruments, and to collect data over specific targets (e.g. hurricanes). A new system is currently under development entailing the permanent installation of GNSS-R instruments on a commercial fleet of Air New Zealand Q300 regional aircraft. This novel and ambitious concept offers a fascinating and powerful system for the collection of science information over a large spatial region and short temporal scales. Here we present an exploratory analysis meant to quantify the merit of such a system as applied to these regional aircraft. We use simulations of realistic flight paths combined with GNSS orbit information to simulate GNSS-R measurement coverage. Results in this scenario confirm the exciting potential of a next-generation GNSS-R receiver.

Index Terms— GNSS Reflectometry, Bistatic radar

1. BACKGROUND

Global Navigational Satellite System Reflectometry (GNSS-R) utilizes GNSS signals reflected from the Earth to provide a wealth of scientific information. Of the spaceborne GNSS-R systems in operation, NASA's Cyclone Global Navigational Satellite System (CYGNSS) Mission, composed of eight micro-satellites, is the most well-known. Although Airborne GNSS-R/RO systems are also widely used to perform experiments [1-5], unlike spaceborne systems, their employment has always been limited to a small number of flights. Recently, the University of Auckland - in collaboration with Air New Zealand (ANZ), the University of Michigan (UM), and The Ohio State University (OSU) - is exploring a compelling concept involving the permanent deployment of GNSS-R instruments on a fleet of small regional aircraft. The GNSS-R instrument would be the Next-Generation GNSS-R Receiver (NGRx), which is currently finalizing development by UM and OSU as part of a NASA Instrument Incubator Program (IIP). Here, small, aircraft-certified GNSS antennas are mounted on the top and bottom of the aircraft to capture direct-path and reflected-path signals, respectively. A subset of the preliminary analysis, which elucidates the measurement coverage of the GNSS-R instrument, is the subject of this paper.

2. AIRCRAFT FLIGHT PATH ANALYSIS

Figure 1(a) shows a photo of the Air Nelson Bombardier Q300 aircraft under consideration. Currently, 23 of these air-

(a) Air New Zealand Q300 Aircraft

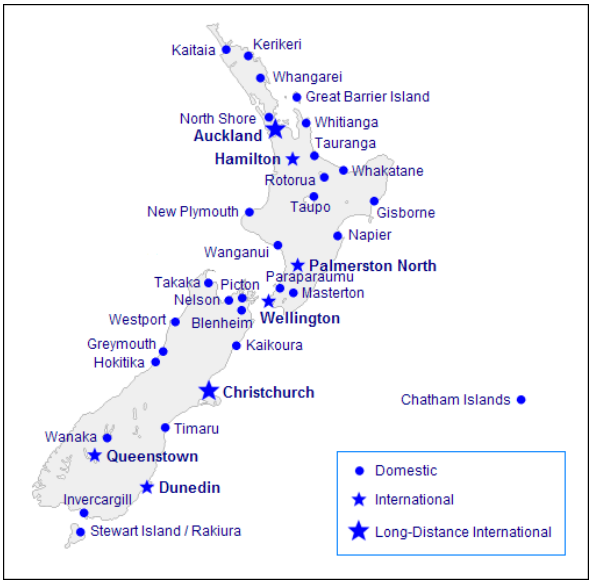

(b) New Zealand Airport Map

Fig. 1: Aircraft under consideration for GNSS-R instrument installation (a) and locations of New Zealand airports (b).

	Auckland	Wellington	Christchurch
Kerikeri	67	0	0
Whangarei	58	0	0
Tauranga	89	55	37
Hamilton	0	14	0
Rotorua	49	45	0
Taupo	33	0	0
Gisborne	73	31	0
Napier	14	55	0
N. Plymouth	59	46	29
Palmerston N.	14	20	0
Nelson	31	134	73
Blenheim	69	66	0
Hokitika	0	0	28
Timaru	0	29	0
Dunedin	0	0	2
Invercargill	0	24	4

Fig. 2: Typical annual routes for a single ANZ Q300 aircraft showing number of flights between New Zealand airports.

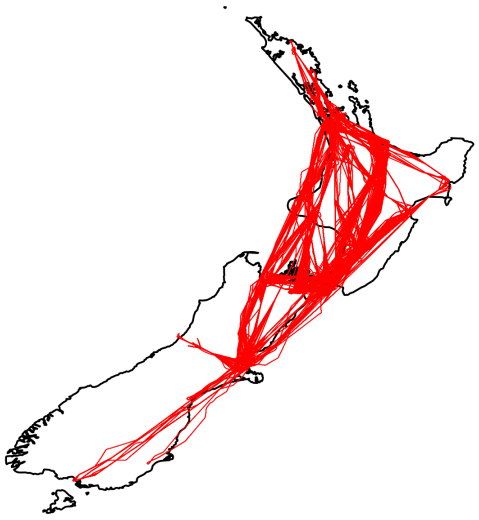

Fig. 3: Flight paths from FlightAware of all ANZ Q-300 aircraft over one week.

craft are in service with this commercial regional air carrier. Figure 1(b) shows a map of New Zealand and the location of the nation's various regional and international airports, with the Q300 fleet operating frequent flights between most (though not all) of them. Table 2 indicates the typical number of annual flights of an individual Q300 craft.

Figure 3 shows the flight paths from of all ANZ Q-300 air- craft over one week. The baseline for the study was an Automatic Dependent Surveillance-Broadcast (ADS-B) dataset detailing the number of Q3000 flights obtained from FlightAware for the week of October 23-30, 2019 [6]. The total number of flights during this week was 1135, which was a particularly busy week given that the estimated annual number of flights for a single Q300 aircraft is around 1268. Thus, for our analysis, the coverage of this one-week period recording the flights of all Q300 aircraft is quite similar to an entire year of flights for a single plane. To condition this data for our GNSS-R simulations, as it contains position and ground speed with an irregular frequency. The flight path data is interpolated to a one-second resolution, and velocity is calculated as a differential position. A criteria of assumptions based on the velocity vector are next used to establish the aircraft attitude frames.

The simulation of GNSS-R measurement coverage assumes the tracking of a single signal type from GPS, Galileo, Beidou, and QZSS constellations [7]. To solve for the specular points, actual flight path data over one week are used to serve as the position and attitude for the receiver, and IGS data provided the transmitter location information. Although acquired measurements are at 1 Hz, the actual rate of the instrument is configurable and will likely be higher.

Figure 4 shows the GNSS-R measurements for the ANZ Q300 aircraft fleet accumulated over 1 week, with measurement binning into 5 km grid cells. Since the number of measurements is very dense near airports (due to the high traffic and low flight altitudes), a log-scale details the measurement count in the figure. Again, note that these results are comparable to the measurements accumulated over a year from just a single Q300 aircraft.

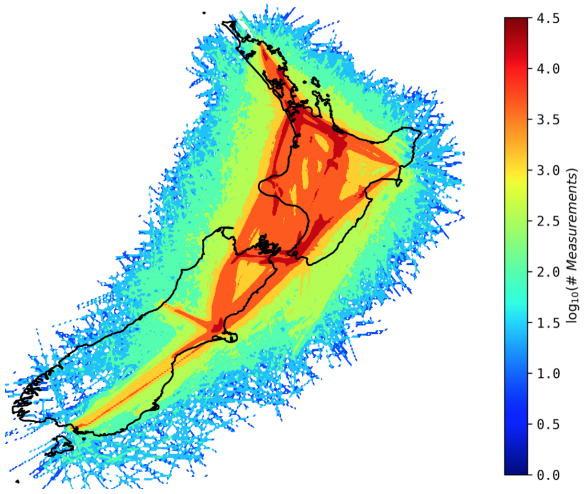

Fig. 4: One week of GNSS-R measurements for the ANZ Q300 aircraft fleet, showing measurement count in log-scale. Results are comparable to a single Q300 aircraft accumulated over a year.

Results indicate that, on average, the duration of each Q300 flight is 45 minutes and accumulates 81,000 measurements. Note also that our simulation does not account for topology, which means that the measurement density over the western mountainous areas are over-represented in this figure. Nonetheless, the coverage and density of measurements

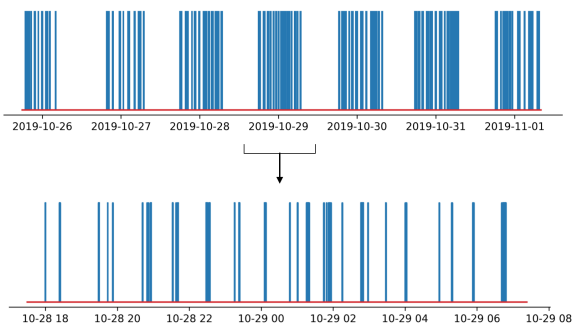

Fig. 5: Temporal sampling of GNSS-R measurements over Lake Taupo versus time (UTC) showing one week (top) and a closer view of a single day (bottom).

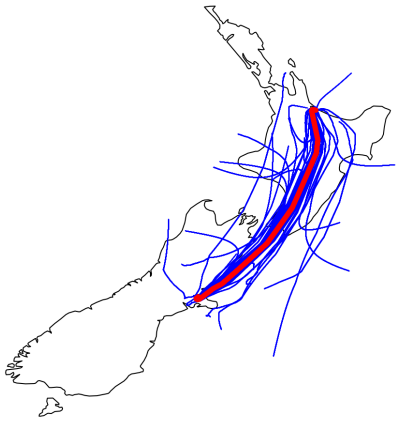

Fig. 6: Example ANZ Q300 flight From Tauranga to Christchurch

is substantial and compelling.

To understand the temporal sampling of a typical area, Figure 5 shows the GNSS-R measurements versus time occurring over Lake Taupo near the center of the North Is- land. As indicated in the top stem sampling plot of the single week of study, regular sampling occurs over the course of a day followed by gaps at night. Note also the magnified results in the lower dataset in Figure 5 detailing the daylight hours of that single 24-hour period, indicating a sub-hourly revisit rate. This behavior, as indicated in the red and orange overlay of the map in Figure 4.

3. ANALYSIS OF A SINGLE FLIGHT

To better elucidate the GNSS-R measurements expected from the system, we will look closer at a single flight, as occurring over Lake Taupo near the center of the North Island. As indicated in the top stem sampling plot of the single week of study, regular sampling occurs over the course of a detailed in Figure 6. The flight path, represented in red, indicates a single ANZ Q300 flight from Tauranga to Christchurch (southward), and the blue lines indicate the locations of GNSS reflection specular points. Results indicate a concentration of measurements around the flight path, with occasional tracks closer to the horizon that are farther away in distance.

In Figure 7, we provide a typical altitude and ground speed profile of a given ANZ Q300 flight, of approximately 20,000 ft. at 250 mph. This flight was 107 minutes in duration with the ascent during departure and descent during approach occupying nearly one third of the flight time.

Figure 8 shows the directions of GNSS satellites over the entire flight in the aircraft body frame. The top plot shows the upper hemisphere and the direction of direct-path signals. The bottom plot shows the lower hemisphere and the directions of reflection-path signals. The azimuth-elevation polar coordinate system indicates the front (F), back (B), left (L) and right (R) of the aircraft. The low altitude of the aircraft

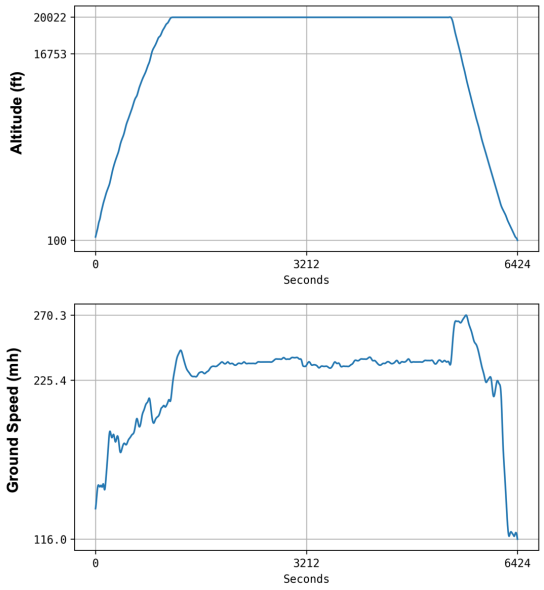

Fig. 7: The altitude and ground speed of the example flight based on ADS-B data.

low altitude as compared to a CYGNSS satellite, results in a nearly mirror image of the directions in the upper and lower hemispheres, with the only noticeable differences occurring near the horizon or with a change in aircraft attitude during ascent and descent phases of the flight. Jagged lines in these plots represent brief adjustments in yaw throughout the flight. Approximate to airports, when the aircraft is within a low altitude profile, the system records measurements quite close to the aircraft location. At cruising altitude, however, the reflections are visible to the horizon at a distance of 278km at an altitude of 20,000 ft.

Figure 9 quantifies the number of available GNSS-R measurements versus time for the GPS and Galileo constellations.

Here, they are divided into three groups based on their incidence angle (as indicated by color). We can see that the majority of measurements have less than a 60 deg. incidence angle, which is the typical range of measurements derived with instruments such as CYGNSS. However, a significant number of higher incidence angles are present within the 60 to 80 degree range, with the incidence of grazing angles prevalent beyond 80 degrees. At these extremes, we expect to observe different behaviors in the GNSS reflection in terms of different polarizations and an increase in coherence.

4. APPLICATIONS

The data provided by the system is expected to enable numerous scientific applications across New Zealand. Since the GNSS-R instrument is capable of wideband, phase and polarimetric measurements, the applications go beyond those provided by current instruments in orbit, such as those aboard CYGNSS. Applications being considered include: measurement of soil moisture and vegetation for agriculture, detection and measurement of inland water level and extent, and measurement of snow pack and ice thickness, and more. Calibration and validation sites are currently being identified, and a comparison to co-located CYGNSS measurements is planned in the Auckland region and Northland. Initial deployment of the instrument aboard the first aircraft is scheduled to take place this year.

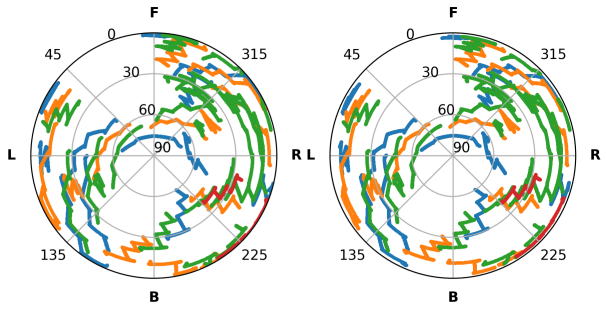

(a) Upper Hem. - Direct Path (b) Lower Hem. - Reflections

Fig. 8: Azimuth and elevation directions to GNSS signals in the aircraft coordinate frame during the example flight for the upward-looking antenna (top) and the downward-looking antenna (bottom).

5. REFERENCES

[1] Garrison, James L. et al. "Effect of sea roughness on bistatically scattered range coded signals from the Global Positioning System," IEEE Geophysical Research Letters, vol 25, no. 30, pg 2257-2260, July 1998.

[2] Lowe, Stephen T. et al. "5-cm-Precision aircraft ocean altimetry using GPS reflections," IEEE Geophysical Research Letters vol 29, no. 10. pg. 1375-1385, May 2002.

[3] Ralf Stosius et al., "GNSS-R Mission Planning Aboard the Research Aircraft HALO," 2010 IEEE Specialist Meeting on GNSS Reflectometry, Barcelona, Spain, October 21-22, 2010.

[4] E. Cardellach et al., "Wetland GNSS-R measurements from aircraft," 2017 IEEE International Geoscience and Remote Sensing Symposium (IGARSS), Fort Worth, TX, 2017, pp. 1122-1125.

[5] F. Xie, J. S. Haase and S. Syndergaard, "Profiling the Atmosphere Using the Airborne GPS Radio Occultation Technique: A Sensitivity Study," in IEEE Transactions on Geoscience and Remote Sensing, vol. 46, no. 11, pp. 3424-3435, Nov. 2008.

[6] FlightAware - Global Flight Tracker Product https://flightaware.com/.

[7] CYGNSS End-to-End Simulator Technical Memo. Space Physics Research Laboratory, 2015. http://clasp-research.engin.umich.edu/missions/cygnss/reference/148-0123 CYGNSS E2ES EM.pdf

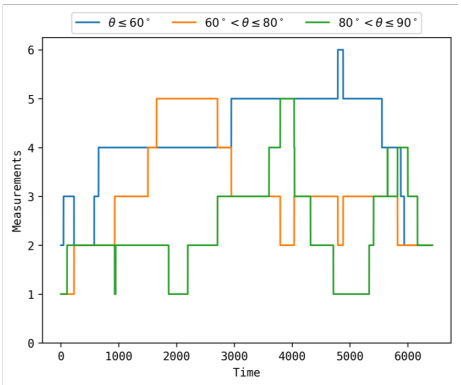

(a) GPS

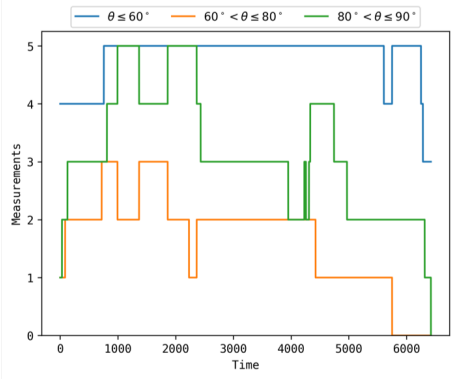

(b) Galileo

Fig. 9: The number of available GNSS-R measurements versus time during the example flight. Results are divided by incidence angle range (θ) separately for the GPS and Galileo constellations.